J Cell Mol Med, 2011, v. 15(12) p. 2684-2696

Cyclic ADP ribose is a novel regulator of intracellular Ca^{2+} oscillations in human bone marrow mesenchymal stem cells

Rong Tao,[1] Hai-Ying Sun,[1] Chu-Pak Lau,[1] Hung-Fat Tse,[1] Hon-Cheung Lee,[2] Gui-Rong Li[1,2]

[1]Department of Medicine, Li Ka Shing Faculty of Medicine, The University of Hong Kong, Pokfulam, Hong Kong SAR, China

[2]Department of Physiology, Li Ka Shing Faculty of Medicine, The University of Hong Kong, Pokfulam, Hong Kong SAR, China

Bone marrow mesenchymal stem cells (MSCs) are a promising cell source for regenerative medicine. However, the cellular biology of these cells is not fully understood. The present study characterizes the cyclic ADP-ribose (cADPR)-mediated Ca^{2+} signals in human MSCs and finds that externally applied cADPR can increase the frequency of spontaneous intracellular Ca^{2+} (Ca^{2+}_i) oscillations. The increase was abrogated by a specific cADPR antagonist or an IP3Rs inhibitor, but not by ryanodine. In addition, the cADPR-induced increase of Ca^{2+}_i oscillation frequency was prevented by inhibitors of nucleoside transporter or by inhibitors of the TRPM2 channel. RT-PCR revealed mRNAs for the nucleoside transporters, CNT1/2 and ENT1/3, IP3R1/2/3, and the TRPM2 channel, but not those for RyRs and CD38 in human MSCs. Knock-down of the TRPM2 channel by specific siRNA abolished the effect of cADPR on the Ca^{2+}_i oscillation frequency, and prevented the stimulation of proliferation by cADPR. Moreover, cADPR remarkably increased phosphorylated ERK1/2, but not Akt or p38 MAPK. However, cADPR had no effect on adipogenesis or osteogenesis in human MSCs. Our results indicate that cADPR is a novel regulator of Ca^{2+}_i oscillations in human MSCs. It permeates the cell membrane through the nucleoside transporters and increases Ca^{2+} oscillation via activation of the TRPM2 channel, resulting in enhanced phosphorylation of ERK1/2 and, thereby, stimulation of hMSC proliferation. This study delineates an alternate signaling pathway of cADPR that is distinct from its well established role of serving as a Ca^{2+} messenger for mobilizing the internal Ca^{2+} stores. Whether cADPR can be used clinically for stimulating marrow function in patients with marrow disorders remains further studied.

Key words: Human bone marrow; mesenchymal stem cells, cyclic ADP-ribose, TRPM2, calcium signaling

Correspondence to: Dr. Gui-Rong Li, L4-59, Laboratory Block, FMB, The University of Hong Kong, 21 Sassoon Road, Pokfulam, Hong Kong SAR China

Tel: 852-2819-9513; Fax: 852-2855-9730; Email: grli@hkucc.hku.hk

J Cell Mol Med, 2011, v. 15(12) p. 2684-2696

Introduction

It is well recognized that bone marrow-derived mesenchymal stem cells (MSCs) are present within the bone marrow cavity and serve as a reservoir for the continuous renewal of various mesenchymal tissues [1-4]. MSCs have recently been moved into the main stream focus by virtue of their plasticity and potential applications in various clinical situations [2, 5], such as tissue regeneration and haematopoietic stem cell transplantation [1, 6]. In addition, MSCs were widely used for the studies of adipogenenic and osteogenenic differentiation [1-4]. However, their cellular biology is not fully understood, especially on the regulation of their cellular activities by the cytosolic free calcium ion (Ca^{2+}_i).

Ca^{2+}_i functions as a highly versatile secondary messenger in virtually all types of eukaryotic cells and regulates a wide range of cellular functions, including the regulation of ion channel, gene transcription, cell proliferation and differentiation [7]. It is generally recognized Ca^{2+}_i are usually mediated by inositol trisphosphate receptors (IP3Rs) and ryanodine receptors (RyRs). Kawano and colleagues were the first to demonstrate that human MSCs exhibit spontaneous Ca^{2+}_i oscillations that are initiated by autocrine/paracrine ATP via the activation of the IP3R-mediated Ca^{2+} release, but not RyRs, since no RyRs are detected in these cells [8-10]. The physiological role of the Ca^{2+} oscillation is unknown but may be important in regulating cellular proliferation. Indeed, it has been reported in other cells that the frequency of Ca^{2+}_i sparks determines the gene expression efficiency [11] and controls kinase activities [12]. Consistently, a recent study demonstrated that the flow stress-manipulated Ca^{2+}_i oscillations in human MSCs can indeed regulate proliferation [13].

Cyclic adenosine diphosphate ribose (cADPR) has been recognized as a universal Ca^{2+} mobilizer by activating RyRs in many types of cells [14-16]. In addition, cADPR has been reported to mediate Ca^{2+} entry by activating transient receptor potential cation channel melastatin-2 (TRPM2) [14, 17, 18]. It plays an important role in the regulation of various cellular behaviors, including insulin secretion [19] and cell proliferation [20]. Cyclic ADP-ribose has been attributed as a non-peptide hematopoietic growth factor because of its unique role in the stimulation of proliferation of human MSCs [21] and its regulation of human hematopoiesis [22-24]. However, the specific mechanism involved is unknown. The present study was thus designed to investigate the mechanism of cADPR in regulating Ca^{2+} signaling in human MSCs during proliferation as well as during adipogenic and osteogenic differentiation. The results from this study demonstrate an alternate signaling pathway of cADPR that is distinct from its well established role of serving as a Ca^{2+} messenger for mobilizing the internal Ca^{2+} stores in human MSCs, which provide important information that human bone marrow function may be regulated by Ca^{2+} signaling.

Materials and methods

Human MSCs culture

Human bone marrow MSCs at passage 1 were generously provided by Dr. Darwin J. Prockop, Texas A&M Health Science Center College of Medicine Institute for Regenerative Medicine at Scott & White. The cells were characterized of positive for surface markers CD44, CD90, CD166, CD105, CD29, CD49c, CD147, CD59 and HLA-1, and negative for CD34, CD36, CD45, CD184 and CD106 (Table S5). These cells have been tested for successful bone and fat differentiation. The cells were cultured at 37°C in 95% air and 5% CO_2, in the growth medium, i.e. minimal essential medium alpha (α-MEM, Invitrogen, Hong Kong) contained 15% fetus bovine serum (Hyclone, Logan, UT, USA), 2 mM glutamine, 100 U/ml penicillin, and 100 μg/ml streptomycin. When cells grew to 70%~80% confluence, they were lifted by 0.25% trypsin and 1 mM ethylene diamine tetraacetic acid (EDTA) in phosphate buffered saline (PBS) solution for subculture as described previously [25].

Differentiation induction

Adipogenesis. Human MSCs were plated into 6-well plates in growth medium and the growth medium was changed to adipogenic medium (α-MEM supplemented with 10% FBS, 1 μM dexamethasone, 0.5 mM 3-isobutyl-1-methylxanthine, 50 μM indomethacin and 10 μg/ml insulin)

J Cell Mol Med, 2011, v. 15(12) p. 2684-2696

when cells reached confluence. After 3 days induction, the adipogenic medium was replaced by maintenance medium (α-MEM supplemented with 10% FBS and 10 μg/ml insulin) and maintained for 2 days. After 2 or 3 cycles of induction and maintenance, plates were fixed with 4% PBS buffered paraformaldehyde solution at 4°C for 1 hour. Followed with washes with PBS to remove paraformaldehyde, Oil red O staining solution was added to visualize the oil drops in differentiated cells.

Osteogenesis. Human MSCs were plated into 6-well plates in growth medium. When cells grew to confluence, the growth medium was changed to osteogenic medium (α-MEM supplemented with 10% FBS, 100 nM dexamethasone, 10 mM beta-glycerol phosphate and 50 μM L-ascorbic acid-2-phosphate). The osteogenic medium was replaced every three days. After 21 days induction, plates were processed to fixation with PBS buffered 4% paraformaldehyde and staining with Alizarin red S for visualization of mineralization [26].

Reverse transcription and polymerase chain reaction

The Reverse transcription and polymerase chain reaction (RT-PCR) was performed as previously described [25, 27, 28]. Briefly, total RNA extraction was performed with Trizol extraction system. RNA pellet was obtained by centrifuge and total RNA was treated with DNase I (GE Healthcare, Hong Kong) to remove genomic DNA at 37°C for 30 minutes. RT was performed with the Promega Reverse Transcription System in a 20-μ1 reaction mixture. The cDNA product from RT reaction was used for PCR amplification of specific gene expression.

PCR primers were designed with human genes using Primer Premier 5 software (Premier Biosoft international, Palo Alto, CA, USA) and synthesized at the Genome Research Center at the University of Hong Kong. The forward and reverse PCR oligonucleotide primers chosen to amplify the cDNA are listed in (Table S1-S3). PCR was performed using a Promega PCR system with Taq polymerase and accompanying buffers. The thermal cycling conditions were: 94°C for 2 min, 28-30 cycles of 94°C (45 s), 58°C (45 s), and 72°C (1 min). This was followed by a final extension at 72°C (10 minutes) to ensure complete product extension. The PCR products were then electrophoresed through a 1.5% agarose gel, and the amplified cDNA bands were visualized using ethidium bromide staining and imaged using Chemi-Genius Bio Imaging System (Syngene, Cambridge, UK).

Western blot

Western blot was performed as previously described [27]. Briefly, Cells at 70~80% confluence were lysed with a modified RIPA buffer containing (in mM) 50 Tris-HCl, 150 NaCl, 1 EDTA, 1 PMSF, 1 sodium orthovanadate, 1 NaF, 1 μg/ml aprotinin, 1 μg/ml leupeptin, 1 μg/ml pepstatin, 1% NP-40, 0.25% sodium deoxycholate, 0.1% SDS. Protein concentration was determined by Bio-Rad protein assay. Cell lysates (50 μg) were mixed with sample buffer and denaturated by heating to 95°C for 5 minutes. Samples were resolved via SDS-PAGE and transferred to nitrocellulose membranes. Membranes were blocked with 5% non-fat milk in TTBS buffer then probed with primary antibodies (1:500-1000) at 4°C overnight with agitation. Anti-Akt, anti-p-Akt, anti-ERK1/2, anti-p-ERK1/2, anti-p38, and anti-p-p38 antibodies were from Millipore (Billerica, MA, USA), while anti-TRPM2 and anti-JNK, anti-PPARγ, and anti-osteocalcin antibodies were from Santa Cruz Biotech (Santa Cruz, CA, USA). After wash with TTBS, the membranes were incubated with HRP-conjugated goat anti-rabbit or donkey anti-goat IgG antibody (Santa Cruz Biotech) at 1:4000 dilutions in TTBS at room temperature for one hour. Membranes were washed again with TTBS then processed to develop x-ray film using an enhanced chemiluminescence detection system (GE Healthcare, Hong Kong). The relative band intensities were measured by quantitative scanning densitometer and image analysis software (Bio-1D, version 97.04, Froebel, Wasserburg, Germany).

$Ca^{2+}{}_i$ measurements

$Ca^{2+}{}_i$ activity was measured using confocal microscopy scanning technique as described previously [29, 30] in human MSCs. The cells were loaded with 5 μM fluo-3 AM (Biotium, Hayward, CA) in the culture medium for 30 min at 37 °C, and then rinsed with PBS to remove extracellular fluo-3 AM

J Cell Mol Med, 2011, v. 15(12) p. 2684-2696

and incubated in Tyrode solution at room temperature for 30 min before recording Ca^{2+}_i signals. Tyrode solution contained (in mM): 140 NaCl, 5.4 KCl, 1 $MgCl_2$, 1.8 $CaCl_2$, 0.33 NaH_2PO_4, 10 HEPES and 10 glucose (pH = 7.3). Ca^{2+}_i was monitored every 10 s in human MSCs using a confocal microscopy (Olympus FV300, Tokyo, Japan) at room temperature (22-23°C). Fluo-3 was excited at 488 nm and emission was detected at >505 nm.

RNA interference

Short interference RNA (siRNA) molecules targeting different exons of TRPM2 gene were synthesized by Ambion Company (Austin, TX). Specific sequences for target genes are shown in Table S4. A FAM-labeled sequence which has no known target in the human genome was used as a negative control (i.e. control siRNA). The siRNA segments (final concentrations at 50 nM as recommended by the supplier) were transfected into human MSCs at 50~60% confluence using lipofectamine 2000 (Invitrogen) as described previously [27] or in supplemental experimental procedures.

Cell proliferation assays

MTT (3-(4,5-dimethyl-thiazol-2-yl)-2,5-diphenyl tetrazolium bromide) assay was applied to assess the effects of ion channel blockers on cell proliferation [27]. Human MSCs were plated into 96-well plate at a density of 5×10^4 cells per well in 200 µl complete culture medium. After 8 h recovery, the culture medium containing ion channel blockers was employed. Following 72 h cADP ribose incubation, 20 µl PBS buffered MTT (5 mg/mL) solution was added to each well and the plates were incubated at 37°C for additional 4 h. The medium was removed and 100 µl/well dimethyl sulfoxide (DMSO) was added to each well to dissolve the purple formazan crystals. The plates were read (wavelengths: test, 570; reference, 630 nm) using a µQuant microplate spectrophotometer (Bio-Tek instruments Inc.). Results were standardized using control group values.

[^{3}H]-thymidine incorporation assay was introduced to assess proliferating cell rate [27]. Human MSCs were plated into 96-well plate at a density of 5×10^4 cells per well in 200 µl complete culture medium. After 8 h recovery, the culture medium was replaced with a medium containing cADP ribose or TRPM2 siRNAs and incubated for 48 h, then 1 µCi (0.037 MBq) ^{3}H-thymidine (GE Healthcare, Hong Kong) was added into each well. Following additional 24 h incubation, cells were harvested and transferred to a nitrocellulose coated 96-well plate via suction. Nitrocellulose membrane was washed with water flow and plate was air dried at 50°C overnight. Liquid scintilla (20 µL per well) was then added to each well. Counts per minute (cpm) for each well was read by a TopCount microplate scintillation and luminescence counter (PerkinElmer, Waltharn, MA).

Statistical analysis

Results are presented as means ± SEM. Paired and/or unpaired Student's t-tests were used as appropriate to evaluate the statistical significance of differences between two group means, and analysis of variance (ANOVA) was used for multiple groups. Values of $P<0.05$ were considered to indicate statistical significance.

Results

Characterization of the human MSCs

Human MSCs (passage 4) showed a fibroblast-like appearance at day 3 after sub-culturing and became confluence at day 8 (Figure 1). Figure 1B and 1C display adipogenic and osteogenic differentiation in human MSCs at passage 5. The cells could be induced to differentiate efficiently into adipocytes (Figure 1B) or osteocytes (Figure 1C), which occurred, however, only after specific induction. RT-PCR (Figure 1D) revealed the expression of lineage specific genes after induction: PPARγ and FABP4 for adipocytes, and RUNX2 and osteocalcin for osteocytes [2, 31]. The PCR primers used for detection of these specific genes are shown in Table S1. These results indicate that

J Cell Mol Med, 2011, v. 15(12) p. 2684-2696

human MSCs we studied here are maintained in the "stem" state before induction.

We found that the amplitude (1-3 arbitrary units) and frequency (oscillation/2.5-13 min) of the spontaneous Ca^{2+}_i oscillations were variable from cell to cell (Figure 1E and 1F). The percentage of human MSCs exhibiting spontaneous Ca^{2+}_i oscillations varied between 86% (110 of 128 cells) in passage 2 cells and 78% (100 of 128 cells) in passage 5 cells (Figure 1G). The percentage was further reduced to only 12.5% at passage 10 (6 of 128 cells, data not shown), which is most likely related to cell senescence in culture [32-34]. Therefore, only human MSCs at passages 2-5 were used in all subsequent experiments.

Spontaneous Ca^{2+}_i oscillations in human MSCs were not related to RyRs [8]. Here, we further confirmed that the spontaneous Ca^{2+}_i oscillations in human MSCs were inhibited by the IP3 inhibitor, 2-aminoethoxydiphenyl borate, the SERCA inhibitor, cyclopiazonic acid, and the SOC channel inhibitor, La^{3+}, but not by ryanodine (Figure S1A-D). Moreover, RT-PCR also revealed the expression of three types of IP3Rs (1/2/3), SERCAs (1/2/3), PMCAs (1/2/3), and NCX (1/3/4) in human MSCs, but not RyRs (Figure S1E and S1F).

Cyclic ADP ribose and Ca^{2+}_i oscillations in human MSCs

Figure 2A shows that the addition of cADPR (50 μM) to the bath solution did not induce Ca^{2+} changes in the cells exhibiting no spontaneous Ca^{2+}_i oscillations (n = 16). However, cADPR (10 and 50 μM) remarkably enhanced the Ca^{2+}_i oscillation frequency in cells with spontaneous Ca^{2+}_i oscillations (Figure 2B and 2C). 8-Br-cADPR (100 μM), a specific antagonist of cADPR, had no effect on the spontaneous Ca^{2+}_i oscillations, but prevented the enhancing effect of cADPR on the oscillation frequency (Figure 2D). Interestingly, the enhancement of the Ca^{2+}_i oscillation frequency by cADPR was not affected by 30 μM ryanodine (Figure 2E). The IP3Rs blocker [8] 2-aminoethoxydiphenyl borate (50 μM), which is also a blocker of TRPM2 channels [35], fully suppressed the Ca^{2+}_i oscillations and antagonized the enhancement on Ca^{2+}_i oscillation frequency by cADPR (Figure 2F). Therefore, the inhibitory effect could be related at least in part to its action on the TRPM2 channels. Indeed, as will be described in detail below, the TRPM2 channel is likely the target of cADPR instead of the RyRs.

The quantitative data for the effects of cADPR on Ca^{2+}_i oscillatory frequency are summarized in Figure 2G. cADPR at 10 and 50 μM significantly increased Ca^{2+}_i oscillation frequency by 69 ± 19% and 108 ± 25%, respectively ($P<0.05$ *vs* before cADPR). These results suggest that the cADPR-induced increase of Ca^{2+}_i oscillation frequency is dependent on the IP3Rs-mediated pathway, but not that mediated by the RyRs.

Nucleoside transporters are responsible for the transport of cADPR

Previous studies have demonstrated that concentrative nucleoside transporters (CNTs) and equilibrative nucleoside transporters (ENTs) are responsible for the transport of external cADPR into human hematopoietic progenitors [24] and HL-60 cells [36]. To determine whether these nucleoside transporters are present in human MSCs, the related mRNAs were examined by RT-PCR, which showed significant expression of ENT1/ENT2 and CNT1/CNT3 in the cells (Figure 3A). Two other components of the cADPR-pathway were also present in human MSCs, the hexameric hemichannel connexin 43 (Cx43) and the bone marrow stromal cell antigen-1 (BST-1). Cx43 has been demonstrated to mediate the nicotinamide adenine dinucleotide (NAD^+) transport and it is known to be functionally interacting with the multifunctional ecto-enzymes, CD38 and/or BST-1 (also called CD157) in the plasma membrane, both catalyze the synthesis and hydrolysis of cADPR [37]. Indeed, BST-1 (CD157) [38, 39], but not CD38, was strongly expressed in human MSCs (Figure 3A).

Nitrobenzylthioinosine (NBMPR) and dipyridamole were found to block the nucleoside transporters ENTs/CNTs [24, 36]. To investigate whether the nucleoside transporters are involved in the transportation of cADPR, human MSCs were pre-treated with NBMPR (10 nM) or dipyridamole (100 nM), and both were effective in blocking cADPR from stimulating the Ca^{2+}_i oscillation frequency (Figure 3C-3E).

J Cell Mol Med, 2011, v. 15(12) p. 2684-2696

The dependence of the cADPR-effect on the TRPM2 channels

RyR mRNA expression was not found in human MSCs (Figure S1). The negative result is not due to the primers we used for RyRs, because all three types of RyR mRNA were detected in human neuroblastoma cell line SH-SY5Y using the same primers (Figure S1F), as reported previously [40].

To investigate whether TRPM2 channels participate in the cADPR-induced increase of Ca^{2+}_i oscillation frequency, two structurally different inhibitors of the channel, econazole (10 μM) and clotrimazole (10 μM) [41], were tested in human MSCs. Both showed no significant effect on the spontaneous Ca^{2+}_i oscillations, but both effectively prevented the increase of Ca^{2+}_i oscillation frequency induced by cADPR (Figure 4B and 4C). The quantitative results are summarized in Figure 4D. RT-PCR (Figure 4E) showed the presence of the mRNA for the full length form of TRPM2, TRPM2-L, but not short form, TRPM2-S, which was also confirmed by Western blot analysis (Figure 4F) for protein expression in human MSCs. These results suggest that the increased Ca^{2+}_i oscillation frequency by cADPR is most likely mediated by the TRPM2 channels.

To further investigate the involvement of the TRPM2 channel in mediating the cADPR- regulation of the spontaneous Ca^{2+}_i oscillations, siRNA molecules (Table S4) targeting human TRPM2 channel were transfected into MSCs using the lipofectamine 2000 reagent. The transfection efficiency was determined to be >90% at 4 hours after transfection (data not shown). Both the mRNA and protein expression of TRPM2 were remarkably reduced by all three of the TRPM2 siRNA molecules, as compared to the control siRNA (Figure 5A). TRPM2 protein levels were significantly reduced by 75% to 89% with the specific siRNAs (Figure 5B and 5C).

The effect of cADPR on the spontaneous Ca^{2+}_i oscillations was examined in human MSCs transfected with TRPM2 siRNAs. They were not significantly affected by the transfection of either the control siRNA or TRPM2 siRNAs. The percentage (81.3%, 26 out of 32 cells) of cells with Ca^{2+}_i oscillations after transfection was close to that shown earlier without transfection (Figure 1G). However, the cells transfected with TRPM2 siRNA molecules showed no response to cADPR (Figure 5E and 5F), whereas in cells transfected with control siRNA, cADPR retained the positive regulatory effect on the Ca^{2+}_i oscillation frequency (Figure 5D). The quantitative results are summarized in Figure 5G, which support the notion that cADPR is a modulator of the spontaneous Ca^{2+}_i oscillations in human MSCs, and the effect is mediated by the TRPM2 channels.

The effect of cADPR on the proliferation of human MSCs

Cell proliferation was assessed by the MTT and the ^{3}H-thymidine incorporation assays. Cyclic ADP ribose increased cell proliferation in a concentration-dependent manner and significant effects were observed at concentrations from 10 to 50 μM (Figure 6A). At 50 μM, the cell proliferation was increased by 19 ± 7% as determined by the MTT assay. The effect was completely antagonized by co-administration of 100 μM 8-Br-cADPR (Figure 6A). Likewise, ^{3}H-thymidine incorporation was increased by cADPR in a concentration-dependent way. At 50 μM, DNA synthesis was enhanced by 32 ± 9% and the effect was fully countered by co-application of 8-Br-cADPR as well (Figure 6B). Consistently, the increase in the rate of DNA synthesis by cADPR was not observed in cells transfected with the TRPM2 siRNAs (Figure 6C), whereas the effect was still seen in the cells transfected with the control siRNA ($n = 10$, $P<0.01$). These results indicate that the enhanced cell proliferation by cADPR is mediated by the TRPM2 channel.

The intracellular mechanism of the cADPR-induced cell proliferation

To determine whether the cADPR-induced increase of proliferation is mediated by MAP kinases, we investigated the phosphorylated levels of the extracellular-signal-regulated kinases1/2 (ERK1/2) and p38 MAP, and survival kinase Akt. Figure 7 A shows that a 30-min incubation with cADPR (10 and 50 μM) increased the phosphorylation level of ERK1/2 (Thr185/Tyr187) in human MSCs, and the effect was countered by 8-Br-cADPR (Figure 7A). The effect of cADPR on phosphorylated ERK1/2

J Cell Mol Med, 2011, v. 15(12) p. 2684-2696

was time-dependent. The increase of ERK1/2 phosphrylation level was maximal at 60 min, and the effect remained significant at 180 min (Figure 7B). However, the increase of phosphorylated ERK1/2 by cADPR was remarkably reduced in the cells transfected with molecule A of TRPM2 siRNAs. Cyclic ADPR (50 μM, 60 min incubation) only induced a slight increase of phosphorylated level of ERK1/2 in TRPM2 siRNA (n=3, P=NS) (Figure 7C).

On the other hand, the phosphorylation levels of Akt (Thr308/Ser473), p38 MAPK (Thr180/Tyr182), and JNK (Thr183/Tyr185) were not significantly affected by cADPR (10 or 50 μM) in human MSCs (Figure 7E-7G). These results showed the specificity of the signaling cascade activated by cADPR in human MSCs, linking via ERK1/2, but not Akt, p38 MAPK or JNK. Consistently, it is well known that ERK1/2 is involved in promoting cell proliferation [42].

The lack of effect of cADPR on adipogenesis and osteogenesis in human MSCs

The effect of cADPR on adipogenesis was determined in human MSCs by application of cADPR (50 μM) in the adipogenic induction medium. Three cycles (3 days/cycle) of induction were employed and Oil red O staining performed at each cycle showed an increase of adipogenesis with each cycle, but cADPR had no effect on adipogenesis (Figure S2A), and No difference of PPARγ expression was observed in the differentiated cells treated with and without cADPR application (Figure S2B). The spontaneous Ca^{2+}_i oscillations disappeared as differentiation progressed, and cADPR (50 μM) could not induce Ca^{2+}_i changes before, during and after adipogenesis (Figure S2C).

The effect of cADPR on osteogenesis was determined in human MSCs by application of cADPR (50 μM) in the osteogenic induction medium for 21 days, with fresh medium replacement every 3 days. Mineralization staining with Alizarin red S displayed the increased osteogenesis with prolonged induction time and cADPR again had no significant effect on osteogenesis as compared to the control group (Figure S3A), and no difference of osteocalcin protein expression was observed in the differentiated cells treated with and without cADPR application (Figure S3B). Similar to that observed in adipogenesis, the spontaneous Ca^{2+}_i oscillations disappeared after osteogenesis, and cADPR (50 μM) could not induce Ca^{2+}_i changes during osteogenesis either (Figure S3B).

Discussion

Cyclic ADP ribose is a well-known endogenous Ca^{2+} mobilizing cyclic nucleotide that targets the intracellular Ca^{2+} stores in the endoplasmic reticulum in many cell types and species covering protozoa, plants and animals, including humans [15, 17]. It is formed by ADP-ribosyl cyclases (CD38 and/or BST-1) from NAD^+. Cyclic ADP-ribose has been established as a second messenger for Ca^{2+} signaling in an equally wide range of cell types [14, 15, 17]. Most unexpectedly, in addition to being an intracellular second messenger, cADPR has recently been proposed to function as a non-peptide hematopoietic growth factor stimulating the expansion of human hematopoietic progenitors in an autocrine/paracrine fashion [21, 24, 43]. It is proposed that cells can release cytoplasmic NAD^+ via the connexin 43 hemi-channels, and is converted extracellularly by the ecto- CD38 and/or BST-1 to cADPR. The latter is then transported back into the progenitors by the nucleoside transporters to perform its Ca^{2+} signaling function intracellularly [44]. The results presented in this study are fully consistent with this novel scheme. Hence, we show that external cADPR can increase the frequency of spontaneous Ca^{2+}_i oscillations in human MSCs and stimulate their proliferation. All the components of the autocrine/paracrine-pathway, Cx34, BST-1, CNTs and ENTs are well expressed in the cells (Figure 3A) and blocking the transport function of the nucleoside transporters indeed inhibits the effects of cADPR.

The intracellular target for cADPR is generally believed to be the ryanodine receptors (RyRs) [14, 15, 17]. However, recent studies have demonstrated that TRPM2 channel is also a target of cADPR [18, 45, 46]. In the present study, we did not find functional or molecular evidence for the presence of the RyRs in human MSCs (Figure S1). This is consistent with a previous report [8] and the idea that RyRs

J Cell Mol Med, 2011, v. 15(12) p. 2684-2696

are expressed mainly in differentiated cells, but not in stem cells [47-49].

Our results strongly support the notion that the TRPM2 channel [41] is responsible for mediating the cADPR-induced increase of Ca^{2+}_i oscillation frequency and cell proliferation in human MSCs. First, both the mRNA and protein of TRPM2 are strongly expressed in human MSCs. Second, blocking the TRPM2 channels pharmacologically using clotrimazole or enconazole or knocking down the channel expression specifically using siRNAs, all inhibit the effects of cADPR (Figure 4). Although the effect of cADPR on IP3Rs is likely involved, the efficacy would be weaker than that on TRPM2 channels.

The TRPM2 channel was initially found to be functionally activated by ADP-ribose by gating at NUDT9-H domain of the channel and acting as an intrinsic deactivation mechanism through its breakdown [50]. Further studies show that cADPR can synergize the action of ADP-ribose on TRPM2 channel activation [18]. In Junket lymphocytes, cADPR can actually activate the TRPM2 channel directly and the effect is antagonized by 8-Br-cADPR, but not by the ADP-ribose antagonist, AMP. In addition, 8-Br-cADPR does not counter the activation of TRPM2 channel by ADP-ribose, indicating that cADPR and ADP-ribose have distinct binding sites on the TRPM2 channel [46]. In pancreatic islets, cADPR evokes Ca^{2+} entry and insulin release, and the effect is significantly diminished by the application of specific siRNAs targeting to the TRPM2 channels [45]. Consistently, we show that 8-Br-cADPR inhibits the cADPR effects in a manner similar to that exerted by either the TRPM2 antagonists or the siRNA knock-down, indicating TRPM2 is the specific target of cADPR in human MSCs.

We demonstrate in this study that the functional consequence of the increase in Ca^{2+} oscillations induced by cADPR is the stimulation of cell proliferation. Thus, blocking the enhancing effect of cADPR on Ca^{2+} oscillation using either 8-Br-cADPR or TRPM2 siRNA correspondingly inhibits the stimulation of proliferation (Figure 6), showing the two are causally correlated. This is consistent with previous studies showing that the frequency of Ca^{2+}_i sparks can determine the efficiency of gene expression in T-lymphocytes [11]. Likewise, in human MSCs the flow stress-manipulated Ca^{2+}_i oscillations have been reported to regulate proliferation as well [13]. The resultant effect of the increased Ca^{2+} oscillations appears to be the simulation of the activities of signaling kinases, as shown in HeLa cells [12]. Indeed, we find that cADPR-promoted proliferation of human MSCs is mediated by enhancing phosphorylation of ERK1/2, but not Akt or P38 MAPK (Figure 7). ERK1/2 is involved in promoting cell proliferation [42]. This is consistent with the previous observation that the fluid flow stress-manipulated Ca^{2+}_i oscillations increased cell proliferation is also related to increased phosphorylation of ERK1/2 in human MSCs [13].

In contrast to the positive correlation between enhancement of Ca^{2+} signaling and cell proliferation, we observe that cell differentiation, both adipogenesis and osteogenesis, leads to cessation of Ca^{2+} oscillation. Consistently, cADPR, a Ca^{2+} messenger, also shows no effect on differentiation (Figure S2 and Figure S3). A similar dichotomic relationship between the cADPR-dependent Ca^{2+} signaling and cell proliferation verses differentiation is also observed in PC12 cells. Thus, activation of the cADPR-pathway is shown to simulate proliferation of PC12 cells, while blockage of the pathway accelerates their neuronal differentiation [51].

It is well known that the characteristics is not identical in human MSCs defined by surface markers and cells isolated from different sources and/or different individuals [21, 24, 52-54], and therefore an intrinsic limitation in using the isolated human MSCs should be noted. There are at least two subset populations of human MSCs (e.g. surface marker $CD106^+$ or $CD106^-$) demonstrated by different laboratories [21, 24, 52-54]. The expression of CD106 was found to be restricted to the $MSCA\text{-}1^+$ and $CD56^-$ MSCs subset [52]. The molecular characteristics may be different in these two subset human MSCs. For example, Scarfi and colleagues have demonstrated that the MSCs they used express surface marker CD106 in 34-78% cells and show significant differences from those (only 0.8% MSCs expressing CD106) we used in this study (Table S5). In particular, mRNAs for CD38, RyR1 and RyR3 are detected, and no spontaneous Ca^{2+} oscillations are observed in their MSCs (Scarfi *et al*., 2008). Most importantly, however, despite these differences, both subsets MSCs are responsive to cADPR and show enhanced Ca^{2+} signaling that leads to stimulation of cell proliferation [21],

J Cell Mol Med, 2011, v. 15(12) p. 2684-2696

providing a strong evidence that the cADPR-pathway is of fundamental importance in regulation cell proliferation of human MSCs, independent of the population difference.

It is well recognized that human MSCs are precursors of hemopoietic stroma which plays an essential role in the bone marrow microenvironment by providing hemopoietic progenitors with soluble factors essential to their proliferation and differentiation and by preventing lymphocyte activation [1-4]. MSCs regulate hemopoiesis through the production of both growth-promoting and cytotoxic factors [55, 56] to produce biochemical signals that are produced by MSCs and active on hemopoietic stem cells, which include cADPR [21, 24, 43]. Cyclic ADPR produced by MSCs is clearly a growth-promoter of human MSCs (Figure 6) [21] and hemopoietic progenitors [24, 43].

In the present study, we limited the cell passages 2 to 5, because it has been reported that human MSCs entered senescence and lose multilineage differentiation potency during *in vitro* passaging [32-34], and biological features and gene expression profile in MSCs could vary between early passages and late passages [57]. The cells used in the present study maintained 'stem' capability, which is reflected in the differentiation experiments (Figure 1, Figure S2 & Figure S3).

Collectively, the present study demonstrates that application of cADPR in bath medium positively regulates the frequency of spontaneous Ca^{2+}_i oscillations and cell proliferation in human MSCs. These effects are mediated by the nuclear transporters CNTs and/or ENTs, TRPM2 channel, and the activation of the MAP kinases ERK1/2. Therefore, cADPR is a cell cycling promoter of MSCs by positive regulation of Ca^{2+}_i oscillations. The results suggest that cADPR likely play an essential role in maintaining *in situ* normal function of bone marrow microenvironment in humans. Whether cADPR can be used clinically for stimulating bone marrow function in patients with marrow disorders remains further studied.

Acknowledgment

This study was supported by Grants from the Research Grant Council of Hong Kong (734703M to GRL, 769107M, 768408, and 769309 to HCL, and the group grant 8CRF09 to HFT and GRL). Dr. R. Tao was supported by a postgraduate studentship from the University of Hong Kong. We thank Dr. Darwin J. Prockop at Texas A&M Health Science Center College of Medicine Institute for Regenerative Medicine at Scott & White (through a grant from NCRR of the NIH, Grant #P40RR017447) for providing the human MSCs.

Conflict interest: None is declared.

J Cell Mol Med, 2011, v. 15(12) p. 2684-2696

References

1. **Zou Z, Zhang Y, Hao L, *et al*.** More insight into mesenchymal stem cells and their effects inside the body. *Expert Opin Biol Ther*. 2010; 10: 215-30.
2. **Pittenger MF, Mackay AM, Beck SC, *et al*.** Multilineage potential of adult human mesenchymal stem cells. *Science*. 1999; 284: 143-7.
3. **Ball SG, Shuttleworth CA, Kielty CM.** Platelet-derived growth factor receptors regulate mesenchymal stem cell fate: implications for neovascularization. *Expert Opin Biol Ther.* 2010; 10: 57-71.
4. **Aggarwal S, Pittenger MF.** Human mesenchymal stem cells modulate allogeneic immune cell responses. *Blood*. 2005; 105: 1815-22.
5. **Smits AM, van Vliet P, Hassink RJ, *et al*.**. The role of stem cells in cardiac regeneration. *J Cell Mol Med.* 2005; 9: 25-36.
6. **Liang X, Su YP, Kong PY, *et al*.** Human bone marrow mesenchymal stem cells expressing SDF-1 promote hematopoietic stem cell function of human mobilised peripheral blood CD34(+) cells *in vivo* and *in vitro*. *Int J Radiat Biol.* 2010; 86: 230-7.
7. **Berridge MJ, Lipp P, Bootman MD.** The versatility and universality of calcium signalling. *Nat Rev Mol Cell Biol.* 2000; 1: 11-21.
8. **Kawano S, Shoji S, Ichinose S, *et al.*** Characterization of Ca(2+) signaling pathways in human mesenchymal stem cells. *Cell Calcium*. 2002; 32: 165-74.
9. **Kawano S, Otsu K, Shoji S, *et al*.** Ca(2+) oscillations regulated by Na(+)-Ca(2+) exchanger and plasma membrane Ca(2+) pump induce fluctuations of membrane currents and potentials in human mesenchymal stem cells. *Cell Calcium*. 2003; 34: 145-56.
10. **Kawano S, Otsu K, Kuruma A, *et al*.** ATP autocrine/paracrine signaling induces calcium oscillations and NFAT activation in human mesenchymal stem cells. *Cell Calcium*. 2006; 39: 313-24.
11. **Dolmetsch RE, Xu K, Lewis RS**. Calcium oscillations increase the efficiency and specificity of gene expression. *Nature*. 1998; 392: 933-6.
12. **Kupzig S, Walker SA, Cullen PJ.** The frequencies of calcium oscillations are optimized for efficient calcium-mediated activation of Ras and the ERK/MAPK cascade. *Proc Natl Acad Sci U S A*. 2005; 102: 7577-82.
13. **Riddle RC, Taylor AF, Genetos DC, *et al*.** MAP kinase and calcium signaling mediate fluid flow-induced human mesenchymal stem cell proliferation. *Am J Physiol Cell Physiol*. 2006; 290: C776-84.
14. **Lee HC.** Multiplicity of Ca^{2+} messengers and Ca^{2+} stores: a perspective from cyclic ADP-ribose and NAADP. *Curr Mol Med*. 2004; 4: 227-37.
15. **Lee HC.** Physiological functions of cyclic ADP-ribose and NAADP as calcium messengers. *Annu Rev Pharmacol Toxicol*. 2001; 41: 317-45.
16. **Guse AH.** Regulation of calcium signaling by the second messenger cyclic adenosine diphosphoribose (cADPR). *Curr Mol Med.* 2004; 4: 239-48.
17. **Guse AH.** Biochemistry, biology, and pharmacology of cyclic adenosine diphosphoribose (cADPR). *Curr Med Chem.* 2004; 11: 847-55.
18. **Kolisek M, Beck A, Fleig A, *et al*.** Cyclic ADP-ribose and hydrogen peroxide synergize with ADP-ribose in the activation of TRPM2 channels. *Mol Cell.* 2005; 18: 61-9.
19. **Okamoto H.** The CD38-cyclic ADP-ribose signaling system in insulin secretion. *Mol Cell Biochem.* 1999; 193: 115-8.
20. **Podesta M, Zocchi E, Pitto A, *et al*.** Extracellular cyclic ADP-ribose increases intracellular free calcium concentration and stimulates proliferation of human hemopoietic progenitors. *FASEB J*. 2000; 14: 680-90.
21. **Scarfi S, Ferraris C, Fruscione F, *et al*.** Cyclic ADP-ribose-mediated expansion and stimulation of human mesenchymal stem cells by the plant hormone abscisic acid. *Stem Cells.* 2008; 26: 2855-64.
22. **Zocchi E, Podesta M, *et al.*** Paracrinally stimulated expansion of early human hemopoietic progenitors by

stroma-generated cyclic ADP-ribose. *FASEB J*. 2001; 15: 1610-2.

23. **Podesta M, Pitto A, Figari O, *et al.*** Cyclic ADP-ribose generation by CD38 improves human hemopoietic stem cell engraftment into NOD/SCID mice. *FASEB J*. 2003; 17: 310-2.

24. **Podesta M, Benvenuto F, Pitto A, *et al.*** Concentrative uptake of cyclic ADP-ribose generated by BST-1^{+} stroma stimulates proliferation of human hematopoietic progenitors. *J Biol Chem*. 2005; 280: 5343-9.

25. **Li GR, Sun H, Deng X, *et al.*** Characterization of ionic currents in human mesenchymal stem cells from bone marrow. *Stem Cells*. 2005; 23: 371-82.

26. **Deng XL, Sun HY, Lau CP, *et al.*** Properties of ion channels in rabbit mesenchymal stem cells from bone marrow. *Biochem Biophys Res Commun.* 2006; 348: 301-9.

27. **Tao R, Lau CP, Tse HF, *et al.*** Regulation of cell proliferation by intermediate-conductance Ca2+-activated potassium and volume-sensitive chloride channels in mouse mesenchymal stem cells. *Am J Physiol Cell Physiol*. 2008; 295: C1409-16.

28. **Tao R, Lau CP, Tse HF, *et al.*** Functional ion channels in mouse bone marrow mesenchymal stem cells. *Am J Physiol Cell Physiol*. 2007; 293: C1561-7.

29. **Hu R, He ML, Hu H, *et al.*** Characterization of calcium signaling pathways in human preadipocytes. *J Cell Physiol*. 2009; 220: 765-70.

30. **Chen JB, Tao R, Sun HY, *et al.*** Multiple Ca^{2+} signaling pathways regulate intracellular Ca2+ activity in human cardiac fibroblasts. *J Cell Physiol.* 2010; 223: 68-75.

31. **Krampera M, Pasini A, Rigo A, *et al.*** HB-EGF/HER-1 signaling in bone marrow mesenchymal stem cells: inducing cell expansion and reversibly preventing multilineage differentiation. *Blood*. 2005; 106: 59-66.

32. **Fehrer C, Lepperdinger G.** Mesenchymal stem cell aging. *Exp Gerontol*. 2005; 40: 926-30.

33. **Sethe S, Scutt A, Stolzing A.** Aging of mesenchymal stem cells. *Ageing Res Rev*. 2006; 5: 91-116.

34. **Baxter MA, Wynn RF, Jowitt SN, *et al.*** Study of telomere length reveals rapid aging of human marrow stromal cells following in vitro expansion. *Stem Cells.* 2004; 22: 675-82.

35. **Togashi K, Inada H, Tominaga M.** Inhibition of the transient receptor potential cation channel TRPM2 by 2-aminoethoxydiphenyl borate (2-APB). *Br J Pharmacol.* 2008; 153: 1324-30.

36. **Guida L, Franco L, Bruzzone S, *et al.*** Concentrative influx of functionally active cyclic ADP-ribose in dimethyl sulfoxide-differentiated HL-60 cells. *J Biol Chem*. 2004; 279: 22066-75.

37. **Malavasi F, Deaglio S, Funaro A, *et al.*** Evolution and function of the ADP ribosyl cyclase/CD38 gene family in physiology and pathology. *Physiol Rev*. 2008; 88: 841-86.

38. **Okuyama Y, Ishihara K, Kimura N, *et al.*** Human BST-1 expressed on myeloid cells functions as a receptor molecule. *Biochem Biophys Res Commun.* 1996; 228: 838-45.

39. **Sato A, Yamamoto S, Ishihara K, *et al.*** Novel peptide inhibitor of ecto-ADP-ribosyl cyclase of bone marrow stromal cell antigen-1 (BST-1/CD157). Biochem J. 1999; 337: 491-6.

40. **Laporte R, Hui A, Laher I**. Pharmacological modulation of sarcoplasmic reticulum function in smooth muscle. *Pharmacol Rev*. 2004; 56: 439-513.

41. **Hill K, McNulty S, Randall AD.** Inhibition of TRPM2 channels by the antifungal agents clotrimazole and econazole. *Naunyn Schmiedebergs Arch Pharmacol.* 2004; 370: 227-37.

42. **Mebratu Y, Tesfaigzi Y.** How ERK1/2 activation controls cell proliferation and cell death: Is subcellular localization the answer? *Cell Cycle*. 2009; 8: 1168-75.

43. **Scarfi S, Fresia C, Ferraris C, *et al.*** The plant hormone abscisic acid stimulates the proliferation of human hemopoietic progenitors through the second messenger cyclic ADP-ribose. *Stem Cells.* 2009; 27: 2469-77.

44. **De Flora A, Zocchi E, Guida L, *et al.*** Autocrine and paracrine calcium signaling by the CD38/NAD+/cyclic ADP-ribose system. *Ann N Y Acad Sci*. 2004; 1028: 176-91.

45. **Togashi K, Hara Y, Tominaga T, *et al.*** TRPM2 activation by cyclic ADP-ribose at body temperature is

involved in insulin secretion. *EMBO J.* 2006; 25: 1804-15.

46. **Beck A, Kolisek M, Bagley LA, *et al.*** Nicotinic acid adenine dinucleotide phosphate and cyclic ADP-ribose regulate TRPM2 channels in T lymphocytes. *FASEB J*. 2006; 20: 962-4.

47. **Resende RR, da Costa JL, Kihara AH, *et al.*** Intracellular Ca(2+) regulation during neuronal differentiation of murine embryonal carcinoma and mesenchymal stem cells. *Stem Cells Dev*. 2010; 19: 379-94.

48. **Fu JD, Li J, Tweedie D, *et al.*** Crucial role of the sarcoplasmic reticulum in the developmental regulation of Ca^{2+} transients and contraction in cardiomyocytes derived from embryonic stem cells. *FASEB J*. 2006; 20: 181-3.

49. **Li X, Yu X, Lin Q, *et al.*** Bone marrow mesenchymal stem cells differentiate into functional cardiac phenotypes by cardiac microenvironment. *J Mol Cell Cardiol*. 2007; 42: 295-303.

50. **Perraud AL, Fleig A, Dunn CA, *et al.*** ADP-ribose gating of the calcium-permeable LTRPC2 channel revealed by Nudix motif homology. *Nature.* 2001; 411: 595-9.

51. **Yue J, Wei W, Lam CM, *et al.*** CD38/cADPR/Ca^{2+} pathway promotes cell proliferation and delays nerve growth factor-induced differentiation in PC12 cells. *J Biol Chem*. 2009; 284: 29335-42.

52. **Battula VL, Treml S, Bareiss PM, *et al.*** Isolation of functionally distinct mesenchymal stem cell subsets using antibodies against CD56, CD271, and mesenchymal stem cell antigen-1. *Haematologica*. 2009; 94: 173-84.

53. **Barbero A, Grogan SP, Mainil-Varlet P, *et al.*** Expansion on specific substrates regulates the phenotype and differentiation capacity of human articular chondrocytes. *J Cell Biochem.* 2006; 98: 1140-9.

54. **Lee HJ, Choi BH, Min BH, *et al.*** Changes in surface markers of human mesenchymal stem cells during the chondrogenic differentiation and dedifferentiation processes in vitro. *Arthritis Rheum*. 2009; 60: 2325-32.

55. **Dazzi F, Ramasamy R, Glennie S, *et al.*** The role of mesenchymal stem cells in haemopoiesis. *Blood Rev*. 2006; 20: 161-71.

56. **Phinney DG.** Biochemical heterogeneity of mesenchymal stem cell populations: clues to their therapeutic efficacy. *Cell Cycle*. 2007; 6: 2884-9.

57. **Vacanti V, Kong E, Suzuki G, *et al.*** Phenotypic changes of adult porcine mesenchymal stem cells induced by prolonged passaging in culture. *J Cell Physiol*. 2005; 205: 194-201.

J Cell Mol Med, 2011, v. 15(12) p. 2684-2696

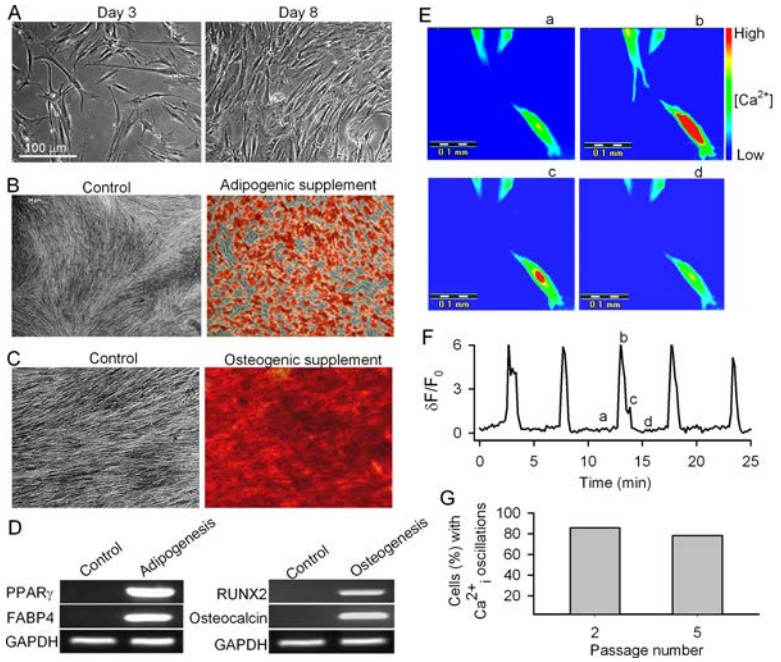

Figure 1. Characteristics of human MSCs. (**A**) Cells in culture on day 3 (left) and day 8 (right) from subculture from passage 4. (**B**) Adipogenic differentiation of human MSCs (passage 5) in control (left) and adipogenic supplement (right). Cells were stained with Oil red O. (**C**) Osteogenic differentiation of human MSCs (passage 5) in control (left) and osteogenic supplement (right). Cells were stained with Alizarin red S. (**D**) RT-PCR revealed the lineage specific genes expression in cells from controls and adipogenic and osteogenic differentiation cultures. PPARγ, peroxisome proliferator-activated receptor gamma; FABP4, fatty acid binding protein 4; RUNX2, runt related transcription factor 2. (**E**) 'Pseudo'-color images show changes in fluorescence intensity (i.e. Ca^{2+}_i) in the cell at time points a, b, c, d, as indicated in F. (**F**) Spontaneous Ca^{2+}_i oscillations observed in a representative cell from passage 3. The pseudo-ratio $\delta F/F_0$: $\delta F/F_0 = (F-F_{base})/F_{base}$ was applied to express Ca^{2+}_i level, where F is the measured fluorescence intensity of Fluo-3, F_{base} is the lowest level of fluorescence intensity in the cell. (**G**) Incidence of spontaneous Ca^{2+}_i oscillations in human MSCs from passages 2 and 5.

J Cell Mol Med, 2011, v. 15(12) p. 2684-2696

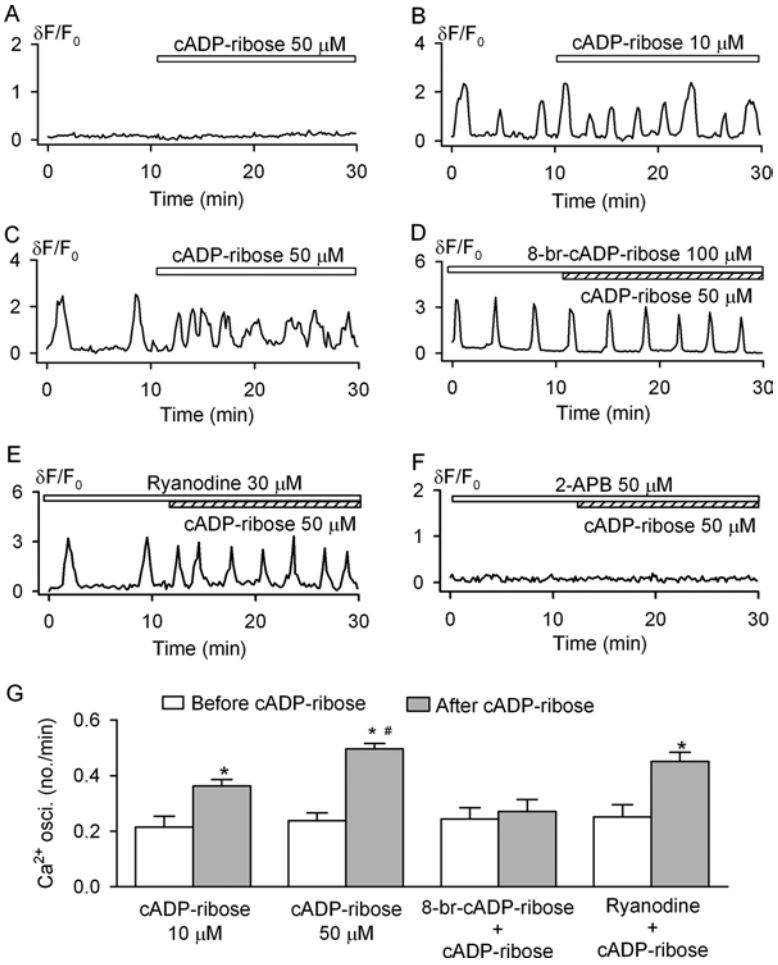

Figure 2. **Effects of cADPR on spontaneous Ca^{2+}_i oscillations**. (**A**) Cyclic ADP ribose did not initiate Ca^{2+}_i transient or Ca^{2+}_i oscillations in the cell without spontaneous Ca^{2+}_i oscillations. (**B** and **C**) Cyclic ADP ribose increased frequency of Ca^{2+}_i oscillations at 10 and 50 μM. (**D**) 8-Br-cADPR prevented the effect of cADPR on Ca^{2+}_i oscillations. (**E**) Ryanodine (30 μM) did not antagonize the cADPR effect. (**F**) IP3Rs blocker 2-APB (50 μM) blocked Ca^{2+}_i oscillations and prevented the cADPR effect. (**G**) Mean values of Ca^{2+}_i oscillation frequencies in the absence or presence of cADPR with under conditions of the effects of 10 μM (n=20), 50 μM (n=36), 100 μM 8-Br-cADPR plus 50 μM cADPR (n=23), and 30 μM ryanodine plus 50 μM cADPR (n=21) on frequency of Ca^{2+}_i oscillations. *P<0.05 *vs* before cADPR, #P<0.05 *vs* 10 μM cADPR.

J Cell Mol Med, 2011, v. 15(12) p. 2684-2696

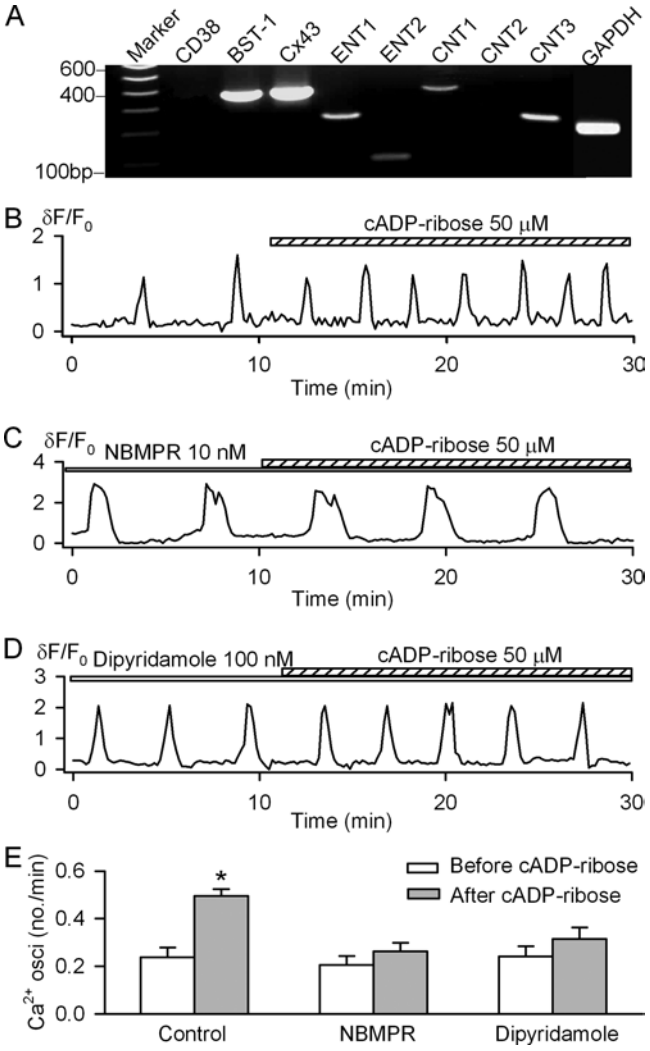

Figure 3. **Nucleoside transporters and cADPR transportation**. (**A**) RT-PCR detected significant gene expression for CNT1, CNT3, ENT1, ENT2, BST-1 and Cx43. No significant CD38 gene expression was detected in human MSCs. CNT: concentrative nucleoside transporter; ENT: equilibrative nucleoside transporter; BST-1: bone marrow stroma antigen-1; Cx43: connexin 43. (**B**) Spontaneous Ca^{2+}_i oscillations in a representative cell. (**C**) cADPR had no significant effect on Ca^{2+}_i oscillations in the cell pretreated with 10 nM NBMPR (nitrobenzylthioinosine). Similar results were obtained in a total of 10 cells. (**D**) The nucleoside transporter inhibitor dypyridamole (100 nM) prevented cADPR effect. (**E**) Mean values for the effects of 50 μM cADPR (n=36), 10 nM NBMPR plus 50 μM cADPR (n=10) and 100 nM dipyridamole plus 50 μM cADPR (n=11) on the frequencies of Ca^{2+}_i oscillations. *P<0.05 *vs* before cADPR.

J Cell Mol Med, 2011, v. 15(12) p. 2684-2696

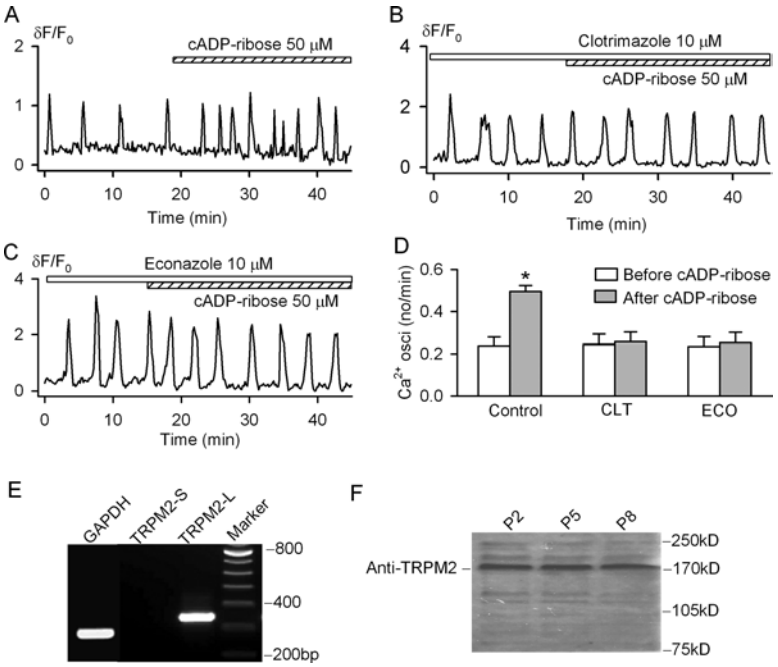

Figure 4. **TRPM2 channel and cADPR in human MSCs.** (**A**) Cyclic ADP ribose increased frequency of Ca^{2+}_i oscillations in a representative cell. (**B**) Cyclic ADP ribose had no significant effect on Ca^{2+}_i oscillations in the cell pretreated with the TRMP2 channel inhibitor clotrimazole. (**C**) Econazole prevented cADPR effect on Ca^{2+}_i oscillations. (**D**) Mean values for the effects of 50 μM cADPR (n=36), 10 μM clotrimazole plus 50 μM cADPR (n=23), and 10 μM econazole plus 50 μM cADPR (n=26) on frequency of Ca^{2+}_i oscillations. *P<0.05 *vs* before cADPR. (**E**) RT-PCR revealed the expression of full length isoform of TRPM2 (TRPM2-L) gene. (**F**) Western blot analysis showed TRPM2 channel protein in human MSCs from passages 2, 5 and 8.

J Cell Mol Med, 2011, v. 15(12) p. 2684-2696

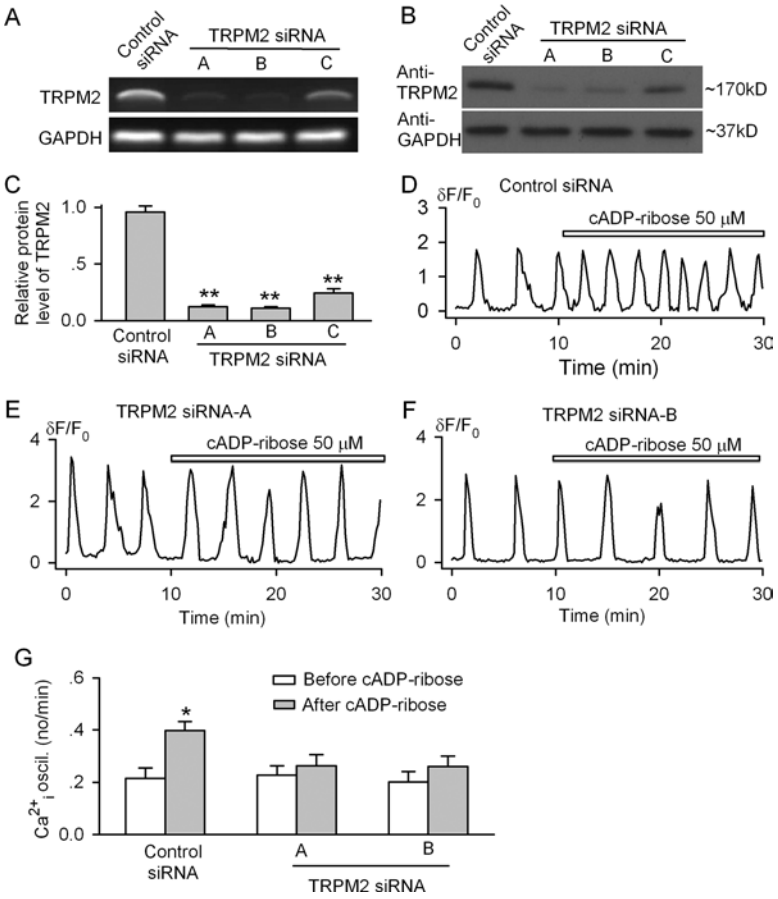

Figure 5. **Knockdown of TRPM2 channel and cADPR effect on Ca^{2+}_i oscillations.** (**A**) RT-PCR images showed the reduced gene expression of TRPM2 channel after transfection with the specific siRNA A, B, and C. (**B**) Western blot analysis showed decreased TRPM2 channel protein by the specific siRNA A, B, and C. (**C**) The mean relative values of TRPM2 channel protein in cells transfected with control siRNA or with the specific siRNAs. n=3, **P<0.01 *vs* control siRNA. (**D**) Cyclic ADP ribose increased the frequency of Ca^{2+}_i oscillations in cells transfected with control siRNA. (**E** and **F**) Cyclic ADP ribose had no effect on Ca^{2+}_i oscillations in cells transfected with TRPM2 siRNA A or B. (**G**) Cyclic ADP ribose increased the frequency of Ca^{2+}_i oscillations in cells transfected with control siRNA. **G:** Mean values for the effects of 50 μM cADPR on frequency of Ca^{2+}_i oscillations in cells transfected with TRMP2 siRNA A (n=26) and B (n=27), and control siRNA (n=25). *P<0.05 *vs* before cADPR.

J Cell Mol Med, 2011, v. 15(12) p. 2684-2696

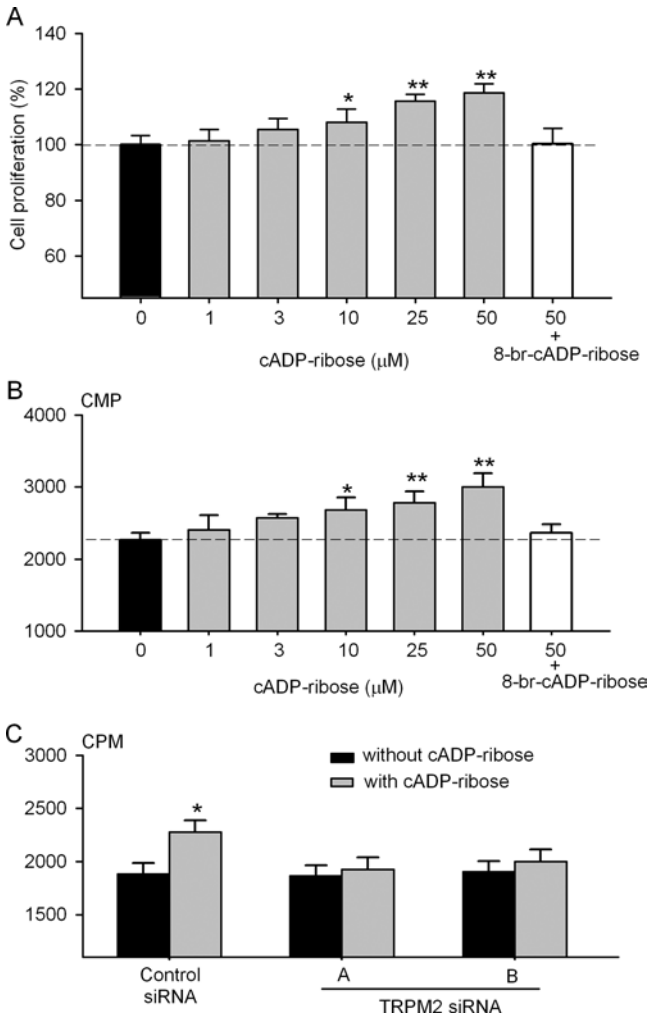

Figure 6. **Effect of cADPR on cell proliferation in human MSCs.** (**A**) Cyclic ADP ribose increased cell proliferation (assessed by MTT assay) in a concentration-dependent manner. The effect was antagonized by 100 μM 8-Br-cADPR. n=10, *P<0.05, **P<0.01 *vs* 0 μM cADPR. (**B**) Cyclic ADP ribose increased ^{3}H-thymidine incorporation in a concentration-dependent manner, and the effect was antagonized by 100 μM 8-Br-cADPR. n =10, *P<0.05, **P<0.01 *vs* 0 μM cADPR. (**C**) Cyclic ADP ribose did not increase ^{3}H-thymidine incorporation in cells transfected with TRMP2 siRNA A or B. n=10, *P<0.05 *vs* without cADPR application.

J Cell Mol Med, 2011, v. 15(12) p. 2684-2696

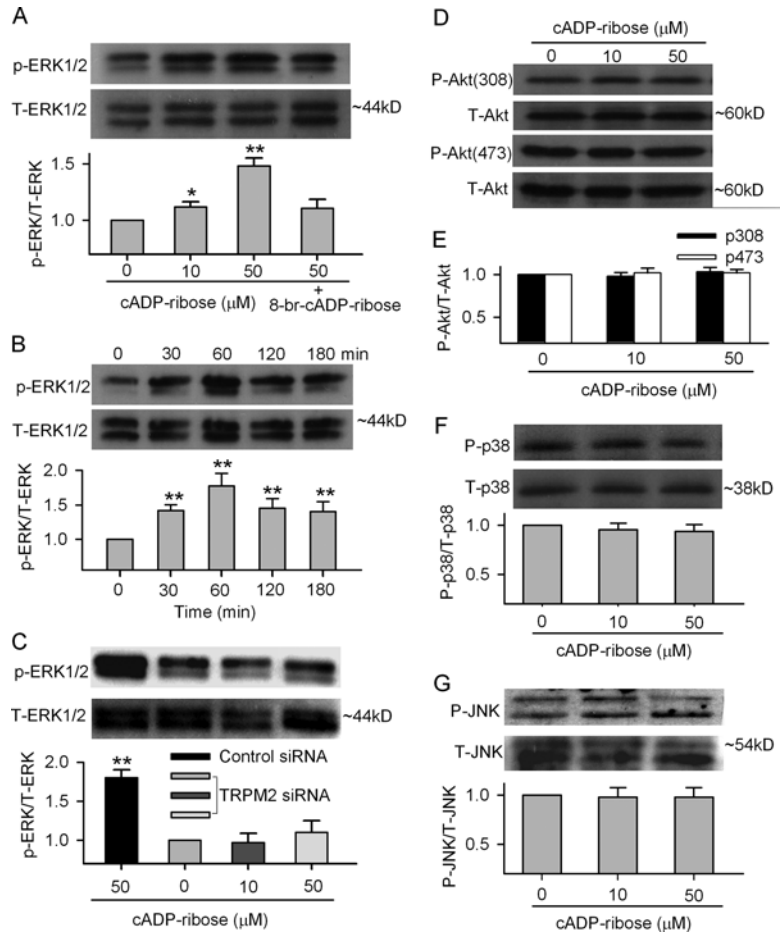

Figure 7. **Cyclic ADP ribose and proliferation-related kinases**. **(A)** ERK1/2 phosphorylation at Thr185/Tyr187 was enhanced in the presence of cADPR (10 and 50 μM) for 60 min and 8-Br-cADPR (100 μM) reduced the effect (upper panels). Mean values (lower panel) for ratio of p-ERK1/2:total ERK1/2 (n=3, *P<0.05, **P<0.01 *vs* 0 μM cADPR). **(B)** Time-dependent effect of cADPR on ERK1/2 phosphorylation and mean values for ratio of p-ERK1/2:total ERK1/2 in the presence of cADPR for 30, 60, 120, and 180 min (n=3, **P<0.01 *vs* 0 μM cADPR). **(C)** ERK1/2 phosphorylation and mean values for ratio of p-ERK1/2:total ERK1/2 in the presence of cADPR in the cells transfected with control siRNA or TRPM2 siRNA for 72 h (n=3, **P<0.01 *vs* 0 μM cADPR). **(D)** Akt1 phosphorylation at Thr308 and Ser473 was not affected by cADPR (10 and 50 μM for 60 min). (**E**) Mean values for ratio of p-Akt(308):total Akt (n=3) and p-Akt(473):total AKT (n=3). (**F**) p38 MAPK phosphorylation levels at Thr180/Tyr182 were not changed when incubated with cADPR (10 and 50 μM) for 60 min (n=3). **(G)** JNK phosphorylation levels at Thr183/Tyr185 were not changed when incubated with cADPR (10 and 50 μM) for 60 min (n=3).